Synthesis of [N(CH3)4]2O3SOSO2(s) and [N(CH3)4]2[(O2SO)2SO2]·SO2(s) containing (SO4)(SO2)x(2−) x = 1, 2, members of a new class of sulfur oxydianions

ARTICLE *in* INORGANIC CHEMISTRY · JUNE 2013

Impact Factor: 4.76 · DOI: 10.1021/ic400805c · Source: PubMed

7 AUTHORS, INCLUDING:

Pablo Bruna
University of New Brunswick
140 PUBLICATIONS **2,868** CITATIONS
SEE PROFILE

F. Grein
University of New Brunswick
245 PUBLICATIONS **3,154** CITATIONS
SEE PROFILE

Juha Mikko Rautiainen
University of Oulu
21 PUBLICATIONS **173** CITATIONS
SEE PROFILE

T.K. Whidden
WhiddenTech
38 PUBLICATIONS **263** CITATIONS
SEE PROFILE

Inorganic Chemistry

Article

pubs.acs.org/IC

Synthesis of $[N(CH_3)_4]_2O_3SOSO_2(s)$ and $[N(CH_3)_4]_2[(O_2SO)_2SO_2]\cdot SO_2(s)$ Containing $(SO_4)(SO_2)_x^{2-}$ x = 1, 2, Members of a New Class of Sulfur Oxydianions

Pablo Bruna,[†] Andreas Decken,[†] Friedrich Grein,[†] Jack Passmore,*[,†] J. Mikko Rautiainen,[‡,∥] Stephanie Richardson,[†] and Tom Whidden[§,⊥]

[†]Department of Chemistry, University of New Brunswick, Fredericton, New Brunswick E3B 5A3, Canada

[‡]Department of Chemistry, University of Oulu, Oulu, P.O. Box 3000, 90014, Finland

[§]Atlantic Hydrogen, Fredericton, New Brunswick E3B 6E9, Canada

Supporting Information

ABSTRACT: One mole equivalent of SO_2 reversibly reacts with $[N(CH_3)_4]_2SO_4(s)$ to give $[N(CH_3)_4]_2S_2O_6(s)$ (**1**) containing the $[O_3SOSO_2]^{2-}$, shown by Raman and IR to be an isomer of the $[O_3SSO_3]^{2-}$ dianion. The experimental and calculated (B3PW91/6-311+G(3df)) vibrational spectra are in excellent agreement, and the IR spectrum is similar to that of the isoelectronic $O_3ClOClO_2$. Crystals of $[N(CH_3)_4]_2(O_2SO)_2SO_2\cdot SO_2$ (**2**) were isolated from solutions of $[N(CH_3)_4]_2SO_4$ in liquid SO_2. The X-ray structure showed that **2** contained the $[(O_2SO)_2SO_2]^{2-}$ dianion. The characterized $N(CH_3)_4^+$ salts **1** and **2** are the first two members of the $(SO_4)(SO_2)_x^{2-}$ class of sulfur oxydianions analogous to the well-known small cation salts of the $SO_4(SO_3)_x^{2-}$ polysulfates.

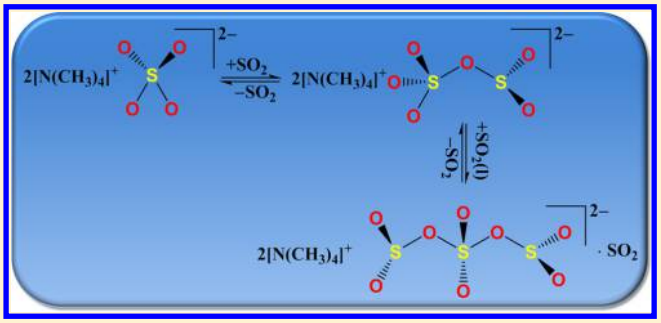

1. INTRODUCTION

The known salts of binary sulfur oxydianions with one to three sulfur atoms were discovered prior to 1891 (Table 1)[1] and are part of the foundational facts of chemistry.[2] Sulfur oxyanions are important in all areas of science and technology, and one would assume that their chemical and physical properties have now been exhaustively established, especially for salts of the first identified hydrated sulfur oxydianion, $[SO_4]^{2-}$.[3] Numerous sulfate salts having small counter cations are stable in the solid state and several are naturally occurring. However, $[SO_4]^{2-}$ undergoes a Coulombic explosion in the gas phase, producing an electron and the $[SO_4]^{-\bullet}$ radical.[4]

In this paper, synthesis of two new sulfur oxidianions, $[O_3SOSO_2]^{2-}$ and $[(O_2SO)_2SO_2]^{2-}$, were obtained by addition of one or two SO_2 to the sulfate dianion. $[O_3SOSO_2]^{2-}$ is an isomer of the long known $[O_3SSO_3]^{2-}$ (Table 1) and isoelectronic with $O_3ClOClO_2$.[5] When compared to sulfate the repulsion between the two negative charges is reduced in $[O_3SOSO_2]^{2-}$ that we surmise is a driving force for reaction 1. In a paper by Chan and Grein,[4] structures and energies of these new dianions were calculated at the B3PW91/6-311+G(3df) level of theory. Accordingly, in the gas phase reactions 1 (formation of $[O_3SOSO_2]^{2-}$) and 2 (formation of $[(O_2SO)_2SO_2]^{2-}$) were calculated to be favorable, with the corresponding ΔG(298 K) [ΔH] values of −174[−211] and −79[−117] kJ mol^{-1}, respectively.

$$[SO_4]^{2-}(g) + SO_2(g) \leftrightarrow [O_3SOSO_2]^{2-}(g)$$
$$\Delta G(298\ \text{K}) = -174\ \text{kJ mol}^{-1} \quad (1)$$

$$[O_3SOSO_2]^{2-}(g) + SO_2(g) \leftrightarrow [(O_2SO)_2SO_2]^{2-}(g)$$
$$\Delta G(298\ \text{K}) = -79\ \text{kJ mol}^{-1} \quad (2)$$

The energetics for the corresponding reactions of solid sulfate salts can be estimated using a Born−Haber cycle for $R_2SO_4(s)$ R = $N(CH_3)_4^+$ and Na^+ (Figure 1). The lattice enthalpies and entropies of solids in the Born−Haber cycle, even for the hitherto unknown salts, are readily estimated from the corresponding molecular volumes using volume based thermodynamics (V.B.T.) (See Supporting Information, Section S1.)[16]

The ΔG values account for the facts that solid Na_2SO_4 does not react with $SO_2(g)$ but the reaction of $SO_2(g)$ with solid $[N(CH_3)_4]_2SO_4$ is energetically favorable as the lattice energy change with the larger cation (76 kJ mol^{-1}) is much smaller than that with Na^+ (296 kJ mol^{-1}) (Figure 1 and the Supporting Information, Section S1). We have further estimated the free energies for reactions of SO_2 with a variety of sulfate salts having differing cation volumes (Supporting Information, Table S1), as well as for the reaction of SO_2 with $R_2O_3SOSO_2$ according to eq 5. These results, shown in Figure

Received: April 2, 2013
Published: June 4, 2013

   dx.doi.org/10.1021/ic400805c | Inorg. Chem. 2013, 52, 7193−7202

Table 1. Known Sulfur Oxydianions Containing One to Three Sulfur Atoms in the Solid State

1		2		3	
anion	discovered [cation] *struct. determination [cation]*	anion	discovered[a] [cation] *struct. determination [cation]*	anion	discovered [cation] *struct. determination [cation]*
		$[O_3S-S]^{2-}$	1799, Chaussie [$2Na^+$] *1952, Taylor* *[$2Na^+$][b]*		
		$[O_2S-SO_2]^{2-}$	1870, Schützenberger [$2Na^+$] *1956, Dunitz* *[$2Na^+$][c]*		
$[SO_3]^{2-}$	1702, Stahl [$2K^+$] *1931, Zachariasen* *[$2Na^+$][d]*	$[O_3S-SO_2]^{2-}$	1797, Vauquelin [$2Na^+$] *1932, Zachariasen* *[$2K^+$][e]*		
		$[O_3S-SO_3]^{2-}$	1819, Gay-Lussac [Mn^{2+}] *1931, Barnes* *[$2K^+$][f]*	$[O_3S-S-SO_3]^{2-}$	1841, Langlois [$2K^+$] *1934, Zachariasen* *[$2K^+$][g]*
$[SO_4]^{2-}$	1625, Glauber [Na^+] *1927, Goeder* *[$2K^+/2Rb^+/2Cs^+$][h]*	$[O_3S-O-SO_3]^{2-}$	1861, Rosenstiehl [$2Na^+/2K^+$] *1960, Truter* *[$2K^+$][i]*	$[O_3SOSO_2OSO_3]^{2-}$	1868, Schultz-Sellack [$2Na^+$] *1954, Eriks* *[$2N_2O_5^+$][j]*
		$[O_3S-O-O-SO_3]^{2-}$	1891, Marshall [$2K^+$] *1934, Zachariasen* *[$2Cs^+/2NH_4^+$][k]*		

[a]Ref 1. [b]Ref 6. [c]Ref 7. [d]Ref 8. [e]Ref 9. [f]Ref 10. [g]Ref 11. [h]Ref 12. [i]Ref 13. [j]Ref 14. [k]Ref 15.

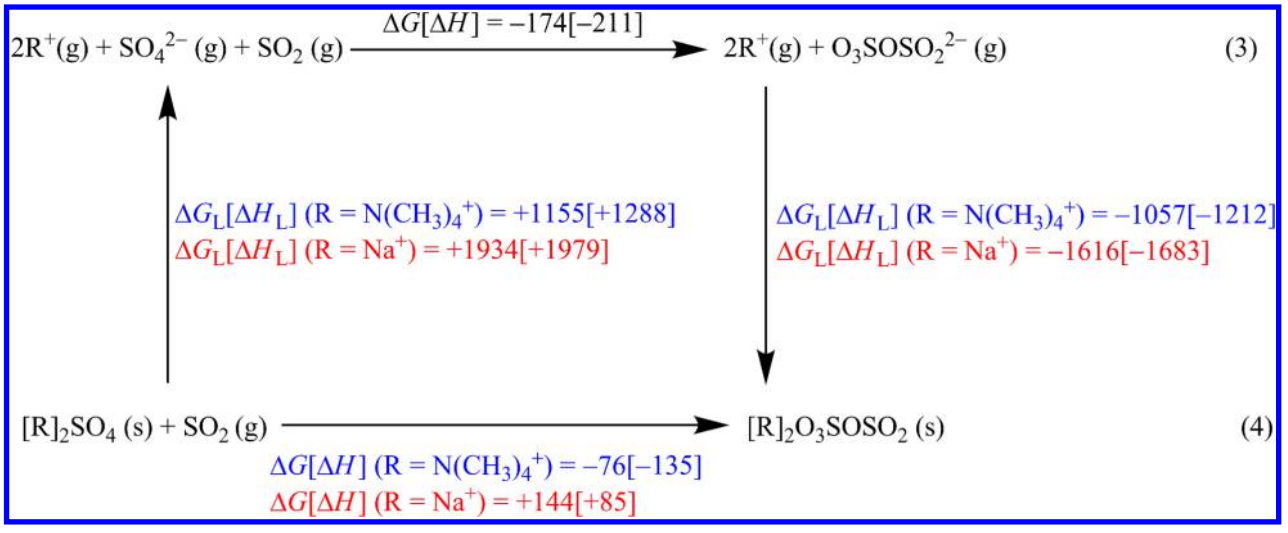

Figure 1. Born−Haber cycle [kJ mol^{-1}] for reaction of $R_2SO_4(s) + SO_2(g)$ where R = $N(CH_3)_4^+$ (blue) and Na^+ (red).

2, suggest that reactions 4 and 5 are favorable for salts of cations having volumes equal to or larger than that of $N(CH_3)_4^+$. Experimental support for the viability of these reactions can be found in a 1938 report by Jander and Mesech[17] that examined the temperature/vapor pressure characteristics of $[N(CH_3)_4]_2SO_4$ with $SO_2(g)$. They reported the formation of two solvates $[N(CH_3)_4]_2SO_4{\cdot}xSO_2$ x = 3, 6, and that the properties of $[N(CH_3)_4]_2SO_4{\cdot}xSO_2$ x = 1, 2 implied a chemical reaction of SO_2 rather than a solvate formation.[17]

$$R_2(O_3SOSO_2)(s) + SO_2(g) \leftrightarrow R_2[(O_2SO)_2SO_2](s) \quad (5)$$

This work is of both fundamental and practical interest. On the fundamental side, the successful preparation of the $N(CH_3)_4^+$ salts of the two novel oxyanions, $[O_2S^{IV}OS^{VI}O_3]^{2-}$ and $[O_2S^{IV}OS^{VI}(O_2)OS^{IV}O_2]^{2-}$, constitutes the discovery of a new class of salts of sulfur oxyanions, $[(SO_4)(SO_2)_x]^{2-}$, analogous to the well-known polysulfates $[(SO_4)(SO_3)_x]^{2-}$ (x = 1−2) given on the addition of xSO_3 to salts of SO_4^{2-} (Table 1)[18] (also known with x = 3 and 4).[19] This work confirms the earlier indications that such compounds exist[17] and is experimental confirmation of the previous computational

dx.doi.org/10.1021/ic400805c | Inorg. Chem. 2013, 52, 7193−7202

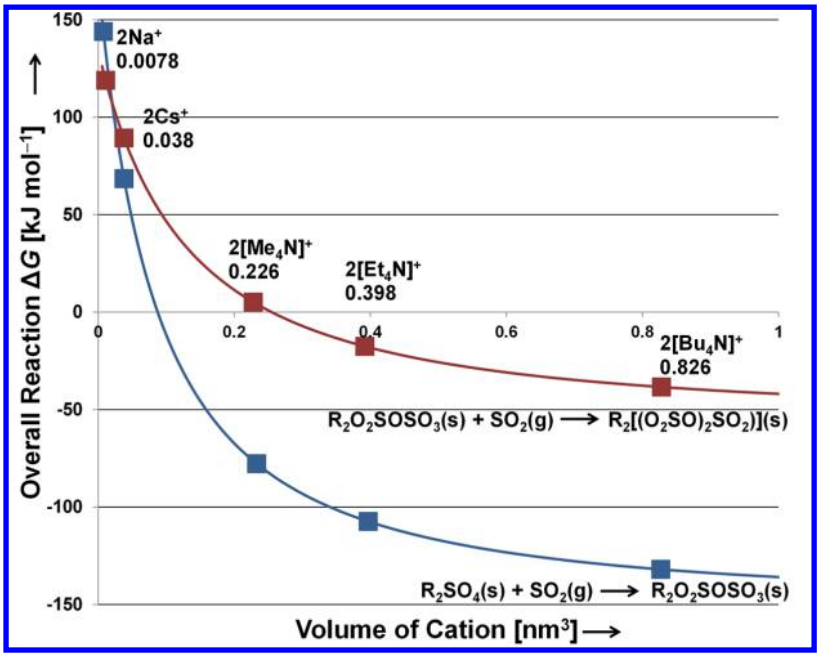

Figure 2. Estimated ΔG_{rxn} (298 K) for reactions 4 and 5 as a function of cation volume.

work by Chan and Grein.[4] Furthermore, our theoretical estimates imply that the chemistry of simple polyanions with large cations may be very different from that of the well-known salts of smaller cations and that stable salts containing numerous new classes of simple binary oxyanions and related anions can be predicted using our methodology and subsequently prepared and studied. Thus preparation of these novel salts constitutes a valuable confirmation of the predictive ability of our methodology.

Within a more practical context, any materials that reversibly absorb and release SO_2 under ambient or near-ambient conditions (i.e., Equations 4 and 5) are of potential industrial interest. Sulfur dioxide is a byproduct of burning fossil fuels, especially coal and emissions of SO_2 produce acid rain that acidifies water resources, degrades monuments and buildings, and harms plant life. The current industrial methods for SO_2 absorption are energetically inefficient, requiring high temperatures for both absorption and regeneration steps. As well, current methods do not capture all of the SO_2, with about 5% released into the air.[20]

This report describes the study of the reaction of $[N(CH_3)_4]_2SO_4(s)$ with various molar equivalents of gaseous SO_2. The solid products of the reaction were characterized by vibrational spectroscopy and by X-ray crystallography.

2. EXPERIMENTAL SECTION

2.1. General Procedures. All solids were manipulated in an MBraun Unilab drybox under a nitrogen atmosphere and/or using a Monel vacuum line and vapor pressure gauge (V = 52 mL). The general techniques have been fully described elsewhere.[21] The reaction vessel used for in situ Raman experiments and for vapor pressure measurements (**A**) was a single 1 cm OD Pyrex tube (V = 14 mL) equipped with a Rotaflo (HP 6K) Teflon-in-glass valve; the vessel used to grow crystals (**B**) was composed of two 3 cm OD Pyrex tubes connected by a medium glass frit to form a H-shaped vessel equipped with two Rotaflo (HP 6K) Teflon-in-glass valves (Supporting Information, Figure S1). Weights were obtained using either a Mettler PM100 balance (0−110 g ± 0.001 g capacity) or a Mettler H311 balance (0−240 g ± 0.0001 g). Vapor pressure measurements were obtained at 20 °C using an Accu-Cal Plus Digital gauge (3D Instruments) with a range of 0−1500 ± 2.5 mmHg.

FT-IR spectra were recorded on a Thermo Nicolet NEXUS 470 FT-IR. Samples were prepared quickly, to minimize decomposition of product, in the drybox, and the spectra obtained as Nujol mulls using KBr plates that were wrapped on the outer edges with Teflon tape. FT-Raman spectra were recorded on a Thermo Nicolet 6700 FT-IR equipped with a Thermo Nicolet NXR FT-Raman accessory at 298 K using a Nd:YVO_4 laser (emission wavelength: 1064 nm; 180° excitation). All Raman spectra were obtained in situ in vessel **A**. Intensities were integrated from the area under the band. Elemental analyses were performed using a LECO CHNS-932 analyzer.

Thermogravimetric analyses (TGA) and differential scanning calorimetry (DSC) were performed on a TA Instruments Q50 analyzer. For TGA, approximately 5 mg of sample was loaded into an Al crucible and crimped with an Al cover in an argon-filled drybox. A pinhole pierced in the cover enabled the escape of SO_2 that evolved during the measurement while minimizing the exposure of the sample to the atmosphere as it was transferred to the TGA instrument. The sample was heated to 500 °C at a ramp rate of 5 °C min^{-1} under a 120 mL min^{-1} N_2 flow. For DSC, 5 mg of material was placed in an Al pan, which was crimped with an Al cover in an argon-filled drybox. The sample pan was mounted on the instrument, and the sample was heated to 500 °C at a rate of 5 °C min^{-1} under a N_2 flow of 95 mL min^{-1}. The reference sample was an empty Al pan containing a cover.

2.2. Materials. Sulfur dioxide (Matheson) was stored over molecular sieves (4 Å) in a 100 mL round-bottom flask (rbf) equipped with a Whitey (1KS4) valve for 24 h and vacuum distilled to a similar rbf and stored over CaH_2 to guarantee that the SO_2 was dry. The SO_2 was degassed using a freeze, pump, thaw method prior to use and was freshly distilled into the reaction vessel via the vacuum line. Tetramethylammonium sulfate (Aldrich, > 99.0%, white free-flowing powder) was used as received. The high purity of the sulfate salt was confirmed by elemental analysis (Found: %C 39.46, %H 9.47, %N 11.27, %S 13.29; Calculated: %C 39.32, %H 9.90, %N 11.46, %S 13.12) and by vibrational spectroscopy, the spectrum was identical to that reported by Malchus and Jansen.[22] Tetramethylammonium sulfate (TCI) was dried under vacuum for 24 h and shown to be spectroscopically (IR and Raman) and analytically less pure (Found: %C 40.19, %H 9.73, %N 11.26, %S 12.50) compared to the Aldrich sample. The Aldrich sample was the preferred sample and was the one used unless otherwise specified. Paratone-N oil (Hampton Research, clear pale yellow oil) was used as received.

dx.doi.org/10.1021/ic400805c | Inorg. Chem. 2013, 52, 7193−7202

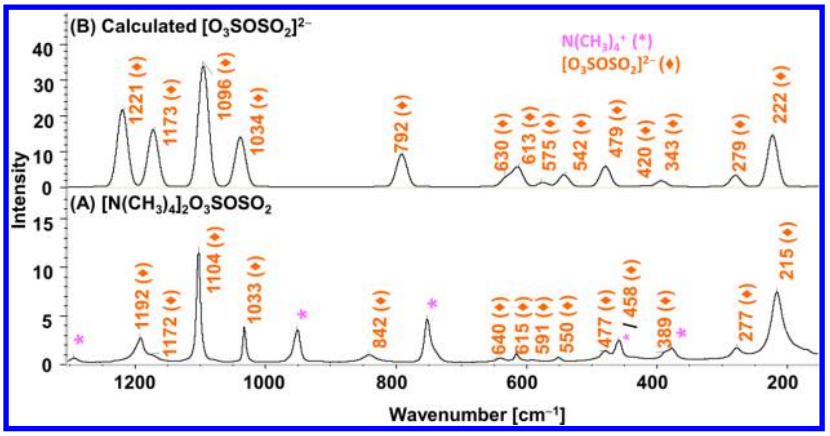

Figure 3. (A) Raman spectrum of $[N(CH_3)_4]_2[O_3SOSO_2](s)$ (**1**) compared with (B) the calculated [B3PW91/6-311+G(3df)] Raman spectrum of $[O_3SOSO_2]^{2-}(g)$ in the 140−1500 cm^{-1} region (2048 scans; 4 cm^{-1} resolution; 0.205 W laser power; Ge detector). Spectrum of the 1500−3500 cm^{-1} region is included in Supporting Information, Figure S2. Assignments related to $N(CH_3)_4^+$ and SO_4^{2-} were made by comparison with those in $[N(CH_3)_4]_2SO_4(s)$ and SO_2 of solvation with similar compounds found in Supporting Information, Table S8.[32]

Table 2. Experimental Vibrational Spectrum of $[O_3SOSO_2]^{2-}$ in 1 [cm^{-1}], Compared with the Calculated (B3PW91/6-311+G(3df)) Spectrum and the Spectrum of the Isoelectronic $O_3ClOClO_2(g)$[5] (Relative Intensities in Brackets)

bands attributed to $[O_3SOSO_2]^{2-}$ in **1**[a]		calculated $[O_3SOSO_2]^{2-}$[a]		$O_3ClOClO_2(g)$[b]	
Raman	IR	Raman	IR	IR	assignments[c]
		35 (1)	35 (<1)		A″
		45 (<1)	45 (1)		A′
		132 (3)	132 (1)		A′ $\nu(O_2S-O)$
215 (84)		222 (42)	222 (13)		A″ $\rho(SO_2)$; $\rho(SO_3)$
277 (15)		279 (9)	279 (<1)		A′ $\rho(SO_2)$; $\rho(SO_3)$
389 (9)	380 (12)	393 (4)	393 (18)		A″ $\delta_{as}(SO_3)$
	429 (3)	420 (1)	420 (<1)		A′ $\delta_s(SO_3)$; $\delta(SO_2)$
477 (10)	476 (9)	479 (17)	479 (40)	544	A′ $\delta(SO_3)$; $\delta(SO_2)$
550 (3)	549 (5)	542 (10)	542 (1)		A″ Rocking (SO_3)
591 (2)	590 (14)	575 (3)	575 (5)	579	A′ $\rho(SO_3)$; $\delta(SO_2)$ $[\nu(O_2S-O)]$
615 (3)	614 (15)	613 (16)	613 (2)	629	A′ $\nu(O_2S-O)$ $[\delta(SOS); \delta_{as}(SO_3)]$
640 (3)	634 (21)	630 (8)	630 (48)	691	A′ $\nu_s(O_3S-O)$
842 (7)	836 (100)	792 (27)	792 (84)	1024	A′ $\nu_s(SO_3)$; $\nu_s(SO_2)$
1033 (9)	1032 (47)	1039 (41)	1039 (53)	1080	A′ $\nu_s(SO_2)$ $[\nu_s(SO_3)]$
1104 (37)	1103 (23)	1096 (100)	1096 (10)		A″ $\nu_{as}(SO_2)$ $[\nu_{as}(SO_3)]$
1172 (3)	1168 (58)	1173 (47)	1173 (45)		A″ $\nu_{as}(SO_3)$
1192 (19)	1210 (87)	1221 (52)	1221 (76)	1265	A′ $\nu_{as}(SO_3)$ $[\nu_{as}(SO_2)]$
1192 (19)	1210 (87)	1222 (12)	1222 (100)	1265	

[a]A full listing of IR and Raman frequencies is given in Supporting Information, Table S2. [b]See Ref 5. No intensities were reported. For a more complete comparison of $[O_3SOSO_2]^{2-}$ and $O_3ClOClO_2$ in the gas phase and solid matrices see Supporting Information, Table S3. [c]Vibrational bands were assigned visually using ChemCraft program; ν - stretching, δ - bending, ρ - twisting/rocking/wagging. Vibration listed first is the main contributor with secondary contribution given in square brackets. Equal contributions are separated by a semicolon.

2.3. X-ray Crystallography. A hemisphere of X-ray diffraction data was collected for crystals of $[N(CH_3)_4]_2[(O_2SO)_2SO_2]\cdot SO_2$ using a Bruker AXS P4/SMART 1000 diffractometer. ω and θ scans had a width of 0.3° and 10 s exposure times. The detector distance was 5 cm. The crystal was twinned and the orientation matrices for two components were determined (CELL_NOW).[23] The data were reduced (SAINT)[24] and corrected for absorption (TWINABS).[25] The structure was solved by direct methods and refined by full-matrix least-squares on F^2 (SHELXTL)[26] on all data. All non-hydrogen atoms were refined using anisotropic displacement parameters. Hydrogen atoms were included in calculated positions and refined using a riding model. The reflections were of weak intensity, and it was not possible to model any disorder in the anion. Figures depicting structures were obtained using Diamond 3.2 program.[27]

2.4. Quantum Chemical Calculations. All calculations were carried out with the Gaussian 03 program package.[28] The B3PW91 functional was used with the 6-311+G(3df) basis set for geometry optimization and frequency calculations.[29] Normal modes were visually assigned using ChemCraft program.[30] There are significant differences between the calculated intensities and the experimental Raman intensities in the region between 1000 cm^{-1} and 1200 cm^{-1} where the calculated intensities are overestimated. Similar discrepancies for the problematic S−O vibrations in this region have been observed in other cases.[31,32] Natural bond orbital analyses were performed with NBO 5.9 program.[33]

2.5.1. In Situ Preparation of $[N(CH_3)_4]_2O_3SOSO_2(s)$ (1). One mole equivalent of $SO_2(g)$ (0.256 g, 4.000 mmol) according to eq 4 (R = $N(CH_3)_4^+$) was expanded into the vacuum line and onto $[N(CH_3)_4]_2SO_4(s)$ (0.970 g, 3.970 mmol) in vessel **A**. The vapor pressure was 1400.0 mmHg, decreasing over 4 h until it equilibrated at 95.0 ± 2.5 mmHg over a partially clumped yellow solid. The remaining SO_2 in the line was condensed into, and isolated in, vessel **A**, the contents agitated by hand and in an ultrasonic bath (20 °C) leading to a free-flowing white homogeneous powder (1.235 g, 4.004

dx.doi.org/10.1021/ic400805c | Inorg. Chem. 2013, 52, 7193−7202

Table 3. Experimental Raman Frequencies Attributed to $[(O_2SO)_2SO_2]^{2-}$ Measured from the Solid Obtained by the Addition of 2.07 mol Equivalents of SO_2 to One Mole of $[N(CH_3)_4]_2SO_4$(s) [cm^{-1}] and Comparison with the Calculated [B3PW91/6-311+G(3df)] Frequencies of $[(O_2SO)_2SO_2]^{2-}$ (Relative Intensities in Brackets)[a]

$[N(CH_3)_4]_2[(O_2SO)_2SO_2]\cdot SO_2$(s) experimental[b]	calculated Raman $[(O_2SO)_2SO_2]^{2-}$ [b]	tentative assignments[c]
169 sh	161 (19)	B $\nu_{as}(O_2S^{VI}(\text{-}OSO_2)_2)$
181 (98)	161 (6)	B $\nu_{as}(O_2S^{VI}(\text{-}OSO_2)_2)$
	232 (4)	A $\rho_t(SO_2)$
242 sh (40)	243 (4)	B $\rho_t(SO_2)$ [$\rho_t(SO_4)$]
342 (<1)	367 (0.8)	A $\delta(SO_4)$ [$\rho_w(SO_2)$]
354 <1)	381 (<1)	B $\rho_w(SO_2)$
459 (24)	398 (1)	A $\delta(SO_4)$ [$\rho_w(SO_2)$]
496 (7)	492 (17)	A $\delta(O_2S^{VI}(\text{-}OSO_2)_2)$ [$\delta(SO_2)$]
544 (5)	541 (<1)	B $\delta(SO_2)$ [$\delta(SO_4)$]
564 (<1)	564 (2)	A $\delta(SO_2)$ [$\delta(SO_4)$]
578 (<1)	586 (8)	A $\delta(SO_4)$ [$\delta(SO_2)$]
593 (<1)	595 (2)	B $\delta(SO_4)$ [$\delta(SO_2)$]
619 (7)	633 (1)	B $\delta(SO_4)$ [$\delta(SO_2)$]
900 (19)	894 (16)	A $\nu_{sym}(SO_4)$ [$\nu_{sym}(SO_2)$]
925 (7)	912 (2)	B $\nu_{as}(SO_4)$ [$\nu_{sym}(SO_2)$]
1124 (100)	1121 (56)	A $\nu_{sym}(SO_2)$; $\nu_{sym}(SO_4)$
	1133 (2)	B $\nu_{sym}(SO_2)$
1145 (64)	1158 (100)	A $\nu_{sym}(SO_4)$ [$\nu_{sym}(SO_2)$]
1238 (5)	1245 (29)	B $\nu_{as}(SO_2)$ [$\nu_{as}(SO_4)$]
1249 (2)	1250 (14)	A $\nu_{as}(SO_2)$ [$\nu_{as}(SO_4)$]
1294 (7)	1288 (26)	B $\nu_{as}(SO_4)$ [$\nu_{as}(SO_2)$]

[a]A full listing of IR and Raman frequencies is given in Supporting Information, Table S4. The observed symmetry is C_1 while that of the calculated anion is C_2 (Figure 8). [b]Ten of the expected 27 vibrations were observed experimentally while eight were calculated [B3PW91/6-311+G(3df)] too low in frequency [12 (A), 13 (B), 29 (A), 48 (B), 110 (A), 110 (B), 161 (A), and 161 cm^{-1} (B)] to be observed. The remaining nine calculated vibrations [169 (B), 342 (A), 354 (B), 459 (A), 496 (A), 564 (A), 578 (A), 593 (B), and 1294 cm^{-1} (B)] had very low calculated intensities and therefore were not observed or were buried in cation or other anion bands. [c]Assignment listed first is the main contributor with secondary contribution given in square brackets. Equal contributions are separated by a semicolon. Bands were assigned visually using ChemCraft; ν- stretching, δ - bending, ρ - twisting/rocking/wagging.

mmol). The vapor pressure measurements were not taken at this point since several experiments showed that the opening and closing of the vessel affected the amount of time it took for the full conversion to the $[O_3SOSO_2]^{2-}$ anion. After a 7 day period in situ Raman spectra showed only bands attributable to **1** (see Figure 3, and Supporting Information, Figures S2 and S3), and vapor pressure dropped to 11.0 mmHg (5−11 mmHg in related experiments). A more detailed account of the preparation of **1** is given in Supporting Information, Section S2.1. The IR spectrum is given in Supporting Information, Figures S4 and S5. A complete vibrational assignment of **1** is given in Supporting Information, Table S2. Vibrations assigned to $[O_3SOSO_2]^{2-}$ have been compared with the experimental IR vibrations of the isoelectronic $O_3ClOClO_2$ and the calculated [B3PW91/6-311+G(3df)] normal modes and intensities of $[O_3SOSO_2]^{2-}$ in Table 2. The TGA and DSC results are given in Supporting Information, Figures S8 and S9, respectively.

2.5.2. Removal of SO_2 from $[N(CH_3)_4]_2O_3SOSO_2$(s). $[N(CH_3)_4]_2O_3SOSO_2$(s) (1.317 g, 4.270 mmol), prepared from $[N(CH_3)_4]_2SO_4$(s) (1.029 g, 4.213 mmol) according to eq 4 (R = $N(CH_3)_4^+$), was subjected to a dynamic vacuum at room temperature. Loss of SO_2(g) was observed by the turbulence of the white powder and weight loss: (0 min/1.317 g, 10 min/1.270 g, 30 min/1.202 g, 50 min/1.129 g, 90 min/1.042 g, 100 min/1.032 g), as illustrated in Supporting Information, Figure S11. After 100 min the Raman spectrum and weight (1.032 g) were, within experimental error, that of the original starting material, $[N(CH_3)_4]_2SO_4$(s) (1.029 g) (Supporting Information, Figure S6). However, we note that samples of $[N(CH_3)_4]_2O_3SOSO_2$(s) (0.149 g) prepared from $[N(CH_3)_4]_2SO_4$(s) (0.116 g) and SO_2(g) (0.033 g) isolated in vessel **A** with the valve closed for 3−4 weeks did not lose weight on pumping for one day, but heating to 100 °C for a few minutes led to SO_2 loss and complete recovery of $[N(CH_3)_4]_2SO_4$(s) (0 min/0.149 g, 10 min/0.119 g), as shown by Raman spectroscopy.

2.5.3. Preparation of Crystals of $[N(CH_3)_4]_2(O_2SO)_2SO_2\cdot SO_2$(s) (2). Crystals of **2** were prepared according to reaction 6. Approximately 13 mol equivalents of SO_2(g) (1.225 g, 19.122 mmol) were condensed directly onto $[N(CH_3)_4]_2SO_4$(s) (0.369 g, 1.510 mmol) in the left-hand side of vessel **B** (Supporting Information, Figure S1). Upon warming to room temperature a yellow solution was formed. The vessel was evacuated by slowly opening the valve on the left-hand side of the vessel under dynamic vacuum. Pumping on the yellow solution gave clear colorless crystals in less than 2 min. The left-hand side of the vessel was isolated as soon as crystals were observed with small amounts of liquid remaining. The vessel was transferred to the drybox and clear, colorless crystals suitable for X-ray diffraction were collected using a spatula tip coated with Paratone-N oil. These crystals were placed in a vial under Paratone-N oil for transportation. The vial lid was wrapped with Teflon tape during transportation. Single crystals coated in Paratone-N oil were mounted using a polyimide MicroMount and cooled to −100 °C in the cold nitrogen stream of the goniometer. Crystallographic details are given in Supporting Information, Table S5.

$$[N(CH_3)_4]_2SO_4(s) + \text{excess } SO_2(l) \leftrightarrow [N(CH_3)_4]_2(O_2SO)_2\cdot SO_2(s) \quad (6)$$

2.5.4. Attempted Preparation of $[N(CH_3)_4]_2(O_2SO)_2SO_2$(s) from $[N(CH_3)_4]_2SO_4$(s) and xSO_2 (x > 2). In accordance with eq 7, 2.07 mol equivalents of SO_2 (0.233 g, 3.637 mmol) were expanded into the vacuum line and condensed at −196 °C onto white $[N(CH_3)_4]_2SO_4$(s) (0.430 g, 1.750 mmol) in vessel **A**. Upon warming to room temperature, a yellow clumped solid was observed. The contents were agitated by hand and in an ultrasonic bath (20 °C), but the powder never became homogeneous.

dx.doi.org/10.1021/ic400805c | Inorg. Chem. 2013, 52, 7193−7202

$$[N(CH_3)_4]_2SO_4(s) + 2SO_2(g) \leftrightarrow [N(CH_3)_4]_2(O_2SO)_2SO_2(s) \quad (7)$$

Several in situ Raman spectra were taken over a period of one month. The bands in the spectrum were assigned to $N(CH_3)_4^+$, $[(O_2SO)_2SO_2]^{2-}$, and additionally to $[O_3SOSO_2]^{2-}$ and SO_2 of solvation (Supporting Information, Figure S7). The observed Raman bands attributed to $[(O_2SO)_2SO_2]^{2-}$ are compared with the calculated [B3PW91/6-311+G(3df)] normal modes and intensities in Table 3. A complete listing of the Raman frequencies has been given in Supporting Information, Table S4. Very similar Raman spectra were obtained from reactions of $[N(CH_3)_4]_2SO_4(s)$ with slightly higher and lower amounts of $SO_2(g)$ than 2 mol equivalents. Bands attributed to $[(O_2SO)_2SO_2]^{2-}$ were also observed in the preparation of $[N(CH_3)_4]_2O_3SOSO_2(s)$ prior to completion of the reaction (Supporting Information, Figure S3).

The addition of 3.3 mol equivalents of SO_2 to $[N(CH_3)_4]_2SO_4(s)$ (0.430 g, 1.750 mmol) in vessel **A** gave a partly yellow and clumped solid. The contents were agitated at room temperature by hand and in an ultrasonic bath (20 °C) but the powder never became homogeneous. In situ Raman spectra of the solids obtained from the reactions $[N(CH_3)_4]_2SO_4 + xSO_2(g)$ x = 2.95, 3.30, 5.50 as a function of time were all similar, except that bands attributed to SO_2 of solvation increased in the intensity as the amount of $SO_2(g)$ reactant increased.

3. RESULTS AND DISCUSSION

3.1. Reversible Absorption of $SO_2(g)$ by $[N(CH_3)_4]_2SO_4(s)$ with Quantitative Formation of $[N(CH_3)_4]_2O_3SOSO_2(s)$ (1). The vapor pressure of one mole equivalent of $SO_2(g)$ over $[N(CH_3)_4]_2SO_4(s)$ dropped first from 1400.0 mmHg (0 h) to 95.0 mmHg (4 h), followed by a much reduced rate of SO_2 uptake until after 7 days the vapor pressure was decreased to about 11.0 mmHg. The resulting white free-flowing powder was unambiguously characterized as $[N(CH_3)_4]_2O_3SOSO_2$ by in situ Raman and IR spectroscopy (see Section 3.3), with the weight gain corresponding to uptake of one mole equivalent of $SO_2(g)$ according to eq 4 (R = $N(CH_3)_4^+$).

SO_2 was quantitatively lost on evacuation of freshly prepared samples, with full recovery of $[N(CH_3)_4]_2SO_4(s)$ (Supporting Information, Figure S6, 1.317 to 1.032 g, theoretical 1.033 g). Periodic in situ Raman spectra of the sample were obtained over time prior to full conversion to **1**. The in situ Raman spectra show strong bands due to the final product and weaker bands attributed to the SO_2 of solvation, $[(O_2SO)_2SO_2]^{2-}$ and SO_4^{2-} (Supporting Information, Figure S3). Attempted optimizations of gas phase $(SO_4)^{2-}\cdot SO_2$ resulted in the covalently bound $[O_3SOSO_2]^{2-}$ structure, suggesting that the SO_2 of solvation is likely associated with **1** and/or $[N(CH_3)_4]_2(O_2SO)_2SO_2(s)$ but not SO_4^{2-}.

3.2. TGA Analysis of 1. The quantitative loss of SO_2 from $[N(CH_3)_4]_2O_3SOSO_2(s)$ on evacuation of the reaction vessel according to eq 4 (R = $N(CH_3)_4^+$) was in line with the thermogravimetric analysis (TGA) and the differential scanning calorimetry (DSC) results of this material that showed the quantitative loss of SO_2 at approximately 90 °C. At temperatures greater than 90 °C the remaining material exhibited characteristics identical to those of $[N(CH_3)_4]_2SO_4$ as reported by Malchus and Jansen[22] (Supporting Information, Figures S8 and S9). The weight loss of a sample of **1** stored in a vial in the drybox was consistent with the loss of SO_2. A TGA of **1** held constant at room temperature over a period of approximately 200 min suggested that SO_2 was gradually released under ambient conditions (Supporting Information, Figure S10).

3.3. Characterization of $[O_3SOSO_2]^{2-}$ in 1 by Vibrational Spectroscopy. The experimental Raman and IR spectra of $[N(CH_3)_4]_2O_3SOSO_2$ (**1**) are given in Figure 3 and Supporting Information, Figure S4, respectively, with frequency assignments attributable to $[O_3SOSO_2]^{2-}$ given in Table 2. Cation bands were assigned by comparison with the previously assigned $N(CH_3)_4^+$ in $[N(CH_3)_4]_2SO_4$.[22] The experimental data related to the anion is in good agreement with the calculated values and assignments in Table 2. Eighteen bands are expected to be active in the Raman spectrum of a $[O_3SOSO_2]^{2-}$ anion having C_s symmetry, of which fifteen were observed in the experimental spectrum. The remaining three bands were calculated to be very weak in intensity or in the low unobservable frequency range. Similar results were seen in the IR, as shown in Supporting Information, Figure S4 and Table 2. The spectra of $[O_3SOSO_2]^{2-}$ contain more bands, and the bands are very different from those reported for the well-known dithionate anion, $[O_3SSO_3]^{2-}$,[34,35] which is calculated to be 53 kJ mol^{-1} lower in energy [B3PW91/6-311+G(3df)]. The IR bands assigned to $[O_3SOSO_2]^{2-}$ are in line with the values reported for the isoelectronic $O_3ClOClO_2$[5] (Table 2 and Supporting Information, Table S3), further supporting the anion identification.

3.4. Structure and Bonding in $[O_3SOSO_2]^{2-}$. The excellent agreement between the experimental vibrational spectrum and calculated normal modes of $[O_3SOSO_2]^{2-}$ strongly supports the validity of the calculated [B3PW91/6-311+G(3df)] structure (Figure 4). The calculated bond

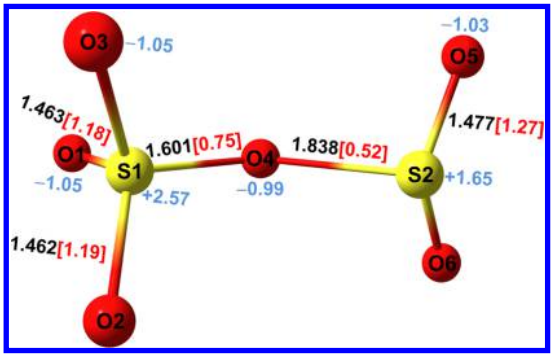

Figure 4. Calculated [B3PW91/6-311+G(3df)] structure of $[O_3SOSO_2]^{2-}$ in the gas phase; bond lengths (black) [Å], Wiberg bond indices (red), and Natural atomic charges (blue).[39] ∠O2−S1−O1: 113.06, ∠O1−S1−O3: 113.06, ∠O3−S1−O4: 107.29, ∠O4−S1−O2: 107.29, ∠S1−O4−S2: 121.88, ∠O4−S2−O6: 100.26, ∠O6−S2−O5: 111.40, and ∠O5−S2−O4: 100.26°.

lengths, angles, Wiberg bond indices, and natural atomic charges in $[O_3SOSO_2]^{2-}$ are in line with those calculated for related species, SO_2, SO_4^{2-}, and $[O_2SOH]^-$ (Figure 5) and show the expected trends. We note that salts of $[O_2SOH]^-$ are unknown, but evidence has been provided that it exists in aqueous solutions.[36] The bridging S−O bonds in $[N(CH_3)_4]_2O_3SOSO_2$ are longer than most other known S−O bonds as shown in Supporting Information, Figure S12, but shorter than those found in some cyclic structures, for example, 1,6-Dioxa-6a-thiapentalene [1.866(2) Å][37] and donor−acceptor adducts, for example, 1,4-dioxane adduct of SO_3, $C_4H_8O_2\cdot SO_3$ [1.861(2) Å].[38]

The current view of the bonding in SO_4^{2-} is that S−O bonds are single σ bonds with high ionic contributions[42] in contrast to earlier views that included double bond character to S−O

dx.doi.org/10.1021/ic400805c | Inorg. Chem. 2013, 52, 7193−7202

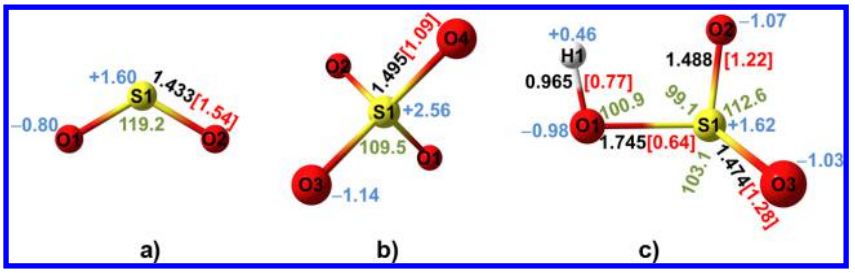

Figure 5. Comparison of calculated [B3PW91/6-311+G(3df)] bond lengths, bond angles, Wiberg bond indices, and natural atomic charges in (a) SO_2, (b) SO_4^{2-}, and (c) $[HOSO_2]^-$; bond lengths (black) [Å], Wiberg bond indices (red), bond angles (green) [deg], and natural atomic charges (blue).[39] For comparison experimental bond lengths and angles reported for SO_4^{2-} in $[N(CH_3)_4]_2SO_4$ are S−O: 1.461(2) Å, ∠OSO: 109.51(9) and 109.4(2)°[22] and for SO_2(s) are S−O: 1.4299(3) Å, ∠OSO 117.16(3)°.[40] Structure of $[HOSO_2]^-$ has been previously calculated at the B3LYP/6-31G(2df,p) level by Steudel et al.,[41] and they reported the S−O bond lengths to be 1.494, 1.482, and 1.768 Å and the O−H bond length 0.966 Å.

bonds.[43] The bonding description of SO_4^{2-} is in line with the more general trend of emphasizing electrostatic interactions in the bonding explanations of the heteroatom bonds of the heavier main groups elements.[40,44]

The structure of $[O_3SOSO_2]^{2-}$ can be viewed as a donor−acceptor adduct of SO_4^{2-} and SO_2 where lone pair electrons of a negatively charged oxygen atom on the Lewis base SO_4^{2-} are donated to the empty π^* lowest unoccupied molecular orbital (LUMO) orbital of SO_2 (see Figure 6).[31] The formation of a donor−acceptor adduct may account for the observation of $[O_3SOSO_2]^{2-}$ rather than the more stable $[O_3SSO_3]^{2-}$ isomer (−53 kJ mol^{-1} at the B3PW91/6-311+G(3df) level of theory), that would require the breaking of a strong S−O bond and forming of an S−S bond. In $[O_3SOSO_2]^{2-}$ 0.41 electrons have been transferred from SO_4^{2-} to SO_2.[45] This process delocalizes the negative charge and contributes to the driving force of reaction 1 as predicted. The charge transfer to SO_2 in $[O_3SOSO_2]^{2-}$ is calculated to be somewhat less than that in $[HOSO_2]^-$ (0.48 electrons) making SO_4^{2-} a weaker base toward SO_2 than OH^-.

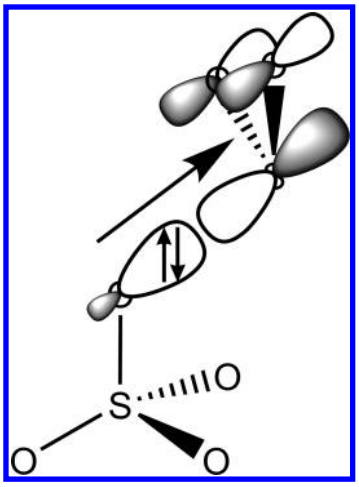

Figure 6. NBO donor−acceptor description of bonding in $[O_3SOSO_2]^{2-}$.[39]

In valence bond terms the structure of $[O_3SOSO_2]^{2-}$ can be represented by a resonance between valence bond structures **A** and **B** shown in Figure 7, where the structure **A** assumes full electron pair donation from SO_4^{2-} to SO_2. The relative weights of **A** and **B** structures can be estimated from the ratios of the bond orders of bridging S−O bonds. The bond order ratio of S1−O4 (0.75) and S2−O4 (0.52) is approximately 3:2 implying the same ratio between the valence bond structures **A** and **B**. Furthermore a similar conclusion can be drawn from the ratio of group atomic charges −1.59 on SO_4 (O1O2S1O3O4) and −0.41 on SO_2 (O5S2O6) moieties in $[O_3SOSO_2]^{2-}$.

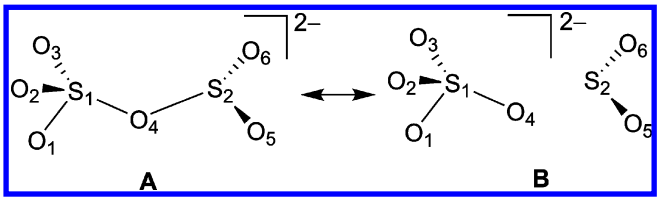

Figure 7. Valence bond description of $[O_3SOSO_2]^{2-}$.

3.5. Preparation of Crystals of $[N(CH_3)_4]_2(O_2SO)_2SO_2{\cdot}SO_2$(s) (2). Single crystals of **2** were obtained from a solution of $[N(CH_3)_4]_2SO_4$ dissolved in liquid sulfur dioxide on removal of the solvent. The structure of **2** was unambiguously determined by X-ray crystallography (Figure 8a). **2** is an SO_2 solvate of the $[(O_2SO)_2SO_2]^{2-}$ dianion and does not contain the discrete isoelectronic $[(O_2SO)_3(SO)]^{2-}$ dianion depicted in Figure 9. We estimate that the formation of $[N(CH_3)_4]_2(O_2SO)_2SO_2$(s) from $[N(CH_3)_4]_2O_3SOSO_2$(s) and SO_2(g) is thermodynamically feasible within the accuracy of our predictive method[46] while the formation of $[N(CH_3)_4]_2(O_2SO)_3(SO)$(s) from $[N(CH_3)_4]_2(O_2SO)_2SO_2$(s) and SO_2(g) is unfavorable (see Supporting Information, Table S1 for details).

The Raman spectrum of very small crystals obtained from the reaction of $[N(CH_3)_4]_2SO_4$ and 2.07 mol equivalents of SO_2 was very similar to those obtained from other reactions with differing molar ratios of the reactants. The main difference in the Raman spectra was the increase in the intensity of SO_2 solvent band as the ratio of SO_2 reactant increased. The peaks in the Raman spectra attributed to $[(O_2SO)_2SO_2]^{2-}$ are compared with the calculated normal modes and intensities in Table 3. We were unable to prepare pure samples of $[N(CH_3)_4]_2(O_2SO)_2SO_2$(s) or $[N(CH_3)_4]_2(O_2SO)_2SO_2{\cdot}SO_2$(s) (**2**). All attempts to prepare the bulk materials gave mixtures as demonstrated by Raman spectroscopy (For example Supporting Information, Figure S7). However, single crystals of **2** have been obtained.

3.6. X-ray Structure of $[N(CH_3)_4]_2(O_2SO)_2SO_2{\cdot}SO_2$(s). The structure of $[N(CH_3)_4]_2(O_2SO)_2SO_2{\cdot}SO_2$(s) consists of discrete $N(CH_3)_4^+$ cations (Supporting Information, Figure S13) and $[(O_2SO)_2SO_2]^{2-}$ anions (Figure 8a) which weakly interact with an SO_2 molecule of solvation to give a two-dimensional sheet (Figure 10).

dx.doi.org/10.1021/ic400805c | Inorg. Chem. 2013, 52, 7193−7202

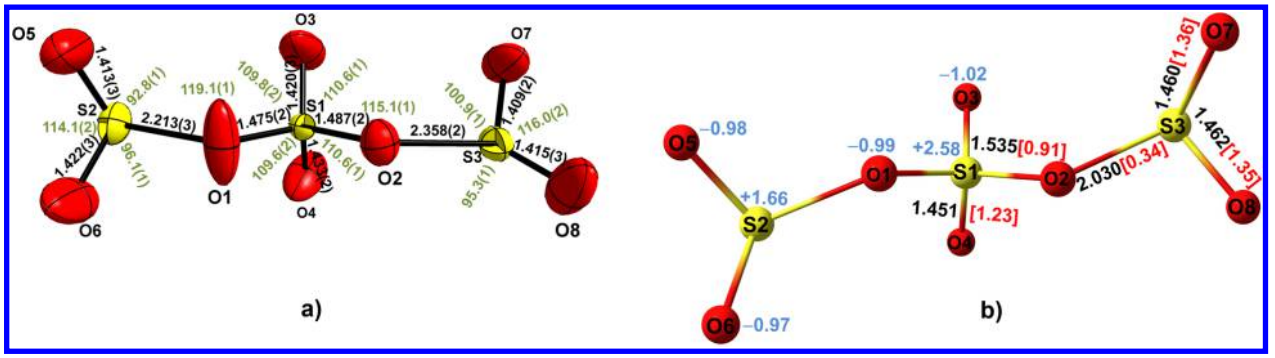

Figure 8. (a) Diamond depiction of $[(O_2SO)_2SO_2]^{2-}$ in **2** (thermal ellipsoid plots are at the 50% probability level) and (b) calculated [B3PW91/6-311+G(3df) level; C_2 symmetry] structure of $[(O_2SO)_2SO_2]^{2-}$ in the gas phase [bond lengths [Å] (black), bond angles [deg] (green), Wiberg bond indices (red), and natural atomic charges (blue)].[39] Selected bond angles for the calculated structure [deg]: ∠O5−S2−O6: 113.1 ∠O6−S2−O1: 101.1, ∠O1−S2−O5: 97.8, S2−O1−S1: 122.6, ∠O1−S1−O3: 109.7, ∠O3−S1−O4: 115.9, ∠O4−S1−O2: 109.7, ∠O2−S1−O1: 105.7, ∠S1−O2−S3: 122.6, ∠O2−S3−O8: 101.1, ∠O8−S3−O7: 113.1, ∠O7−S3−O2: 97.8.

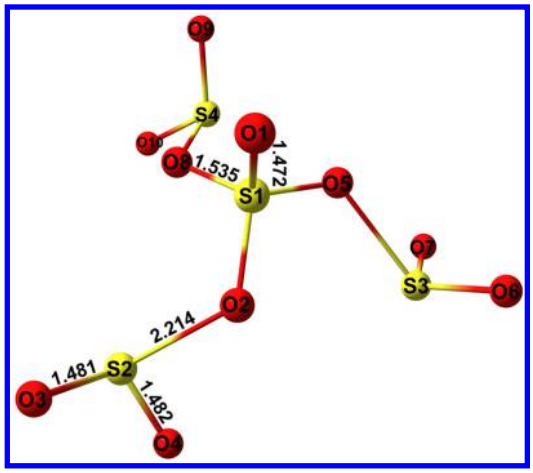

Figure 9. Optimized structure of $[(O_2SO)_3(SO)]^{2-}$ (B3PW91/6-31+G* level; C_3 symmetry) with bond lengths [Å].[4]

The cations reside in between the layers formed by the anions and solvent molecules in the *bc* plane (Supporting Information, Figure S14). The anion and cations are linked by numerous O−H hydrogen bonds (Supporting Information, Table S6). The geometry of $N(CH_3)_4^+$ is very similar to that in $[N(CH_3)_4]_2SO_4$ (Supporting Information, Table S7).[22] The S−O distances in the SO_2 solvent molecule [S4−O10 1.394(4) Å, S4−O9 1.344(4) Å, ∠SOS 120.0(2)°] in **2** are shorter than in SO_2(s) [1.4299(3) Å, ∠SOS 117.16(3)°][40] (Supporting Information, Table S8). Many X-ray structures containing SO_2 fragments often give S−O distances that are much shorter than expected (e.g., see references 31 and 32 and references therein), likely because of unresolved SO_2 disorder and/or unaccounted for librational motion.

3.7. Structure and Bonding in $[(O_2SO)_2SO_2]^{2-}$. Two minimum conformations with almost the same energy (energy difference 2.3 kJ mol^{-1}) were optimized for $[(O_2SO)_2SO_2]^{2-}$. The conformation that more resembled the experimental structure (Figure 8a) is presented in Figure 8b while the other conformation is given in the Supporting Information, Figure S17. The optimized structure of $[(O_2SO)_2SO_2]^{2-}$ can be viewed as being formed by donor−acceptor interactions between SO_4^{2-} and two SO_2 molecules in analogous fashion to $[O_3SOSO_2]^{2-}$ above. The negative charge on the SO_4 moiety in $[(O_2SO)_2SO_2]^{2-}$ (−1.42) is less than in

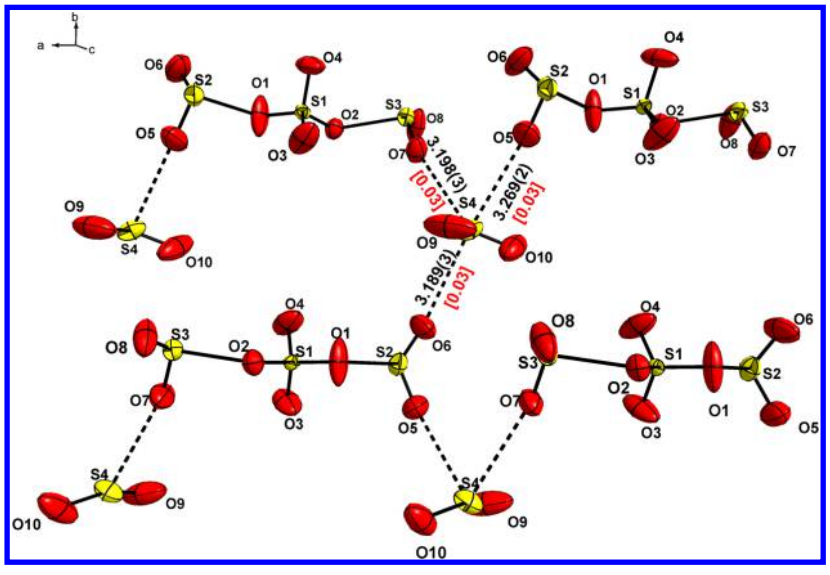

Figure 10. Portion of the layer of $[(O_2SO)_2SO_2]^{2-}$ anions and weakly interacting SO_2 molecules of solvation in the *ab* plane of **2**, bond distances [Å] (black) and bond orders (red)[47] (thermal ellipsoid plots are drawn at the 50% probability level).

dx.doi.org/10.1021/ic400805c | *Inorg. Chem.* 2013, 52, 7193−7202

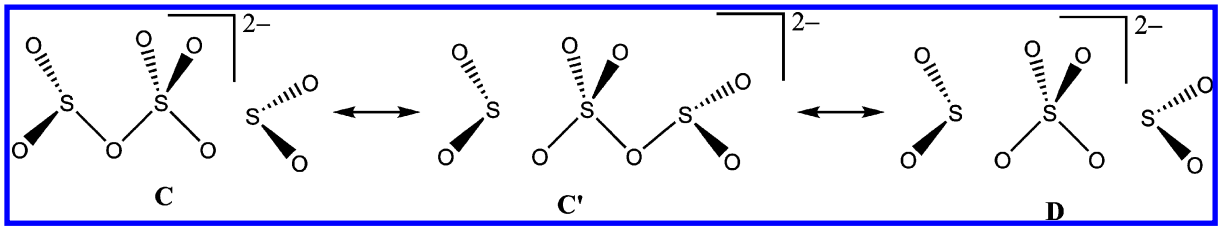

Figure 11. Valence bond description of $[(O_2SO)_2SO_2]^{2-}$.

$[O_3SOSO_2]^{2-}$ (−1.59) and the transfer to the two terminal SO_2 moieties (−0.58) is greater than the negative charge transfer to the single SO_2 in $[O_3SOSO_2]^{2-}$ (−0.41). In addition the negative charge is delocalized over a larger volume. The calculated anion structure can be represented in valence bond terms with resonance structures **C**, **C′**, and **D** (Figure 11). The calculated bridging S2−O1 (2.030 Å, B.O.: 0.34) bond suggests that the relative weights of **C**, **C′**, and **D** structures are close to 1:1:1.

Compared to the optimized structure the interaction between the central SO_4 unit and terminal SO_2 moieties in the experimental X-ray structure is weaker as evidenced by the longer bridging sulfur−oxygen bond lengths S2−O1 (2.213(3) Å, B.O.: 0.31) and S3−O2 (2.358(2) Å, B.O.: 0.22).[47] Despite of the weaker interaction the identity of the anion is judged to remain the same. The only difference is the higher contribution of the nonbonding **D** resonance structure to bonding in the experimental structure compared to the optimized structure. The weaker interaction between the central SO_4 unit and terminal SO_2 moieties in the experimental structure can be attributed to numerous cation−anion H···O interactions (Supporting Information, Table S6) and influence of the SO_2 solvate molecules that are expected to delocalize some of the negative charge on the anion. Compared to the majority of known S−O bonds (Supporting Information, Figure S12) the bridging S−O bonds in $[(O_2SO)_2SO_2]^{2-}$ are long but bonds in the same range (2.00−2.50 Å) have been reported.[48] A related bridging O−SO_2 bond distance that is even longer than those in $[(O_2SO)_2SO_2]^{2-}$ was reported in $[(\eta^6\text{-}C_6H_6)_2Cr]S_2O_6{\cdot}2SO_2$ (2.433(4) Å, B.O. = 0.18).[47,49] The authors formulated the structure as SO_2 solvate, but it can also be viewed as a sulfur oxyanion, $[S_4O_{10}]^{2-}$, that has even greater contribution of a valence bond structure corresponding to a nonbonding resonance form similar to **D** than $[(O_2SO)_2SO_2]^{2-}$. The previously known very long S−O bonds can be regarded either as a part of a bond/no bond resonance system or alternatively as a part of a multicentered σ bond.[50]

4. CONCLUSIONS

We have shown that the use of Born−Haber cycles and volume based thermodynamics to estimate lattice energies with density functional theory (DFT) enthalpies of the corresponding gas phase reactions correctly predicted that $[N(CH_3)_4]_2SO_4$ will react with SO_2 to give $[N(CH_3)_4]_2O_3SOSO_2$ (**1**) and $[N(CH_3)_4]_2(O_2SO)_2SO_2$. Subsequently $[N(CH_3)_4]_2SO_4$ was experimentally shown to reversibly and quantitatively take up gaseous SO_2 at room temperature to produce $[N(CH_3)_4]_2O_3SOSO_2$, an isomer of the known $[O_3SSO_3]^{2-}$ dianion. This salt was unambiguously characterized using vibrational spectroscopy. Crystals of $[N(CH_3)_4]_2(O_2SO)_2SO_2{\cdot}SO_2$ (**2**) were isolated from solutions of $[N(CH_3)_4]_2SO_4$ in liquid SO_2. The X-ray structure of **2** showed that it contained the $[(O_2SO)_2SO_2]^{2-}$ dianion. The $[O_3SOSO_2]^{2-}$ and $[(O_2SO)_2SO_2]^{2-}$ oxydianions are the first new sulfur oxydianions containing one to three sulfur atoms that have been identified since 1891 (Table 1) and are the first members of a new class of $[SO_4][SO_2]_x^{2-}$ (x = 1, 2) sulfur oxyanions, analogous to the well-known series of $SO_4[SO_3]_x^{2-}$ polysulfates (Table 1) isolated as salts of small cations.

This work illustrates the usefulness of predictive thermodynamics and the importance of size in salt reactivity. It implies that the chemistry of oxydianions of sulfur with large cations will be very different from that of the more traditional salts of small cations. This will be further illustrated in upcoming publications. It also implies that the energetics of SO_2 uptake by sulfates can be tailored by changing the size of the cation. This represents a unique opportunity for the engineering of reversible SO_2 uptake reagents.

The present work compliments the classical 1938 studies by Jander and Mesech on the SO_2 uptake by $[N(CH_3)_4]_2SO_4$, and confirms their suggestion that $[N(CH_3)_4]_2SO_4{\cdot}(SO_2)_x$ x = 1 and 2 were not just SO_2 solvates of $[N(CH_3)_4]_2SO_4$.

■ ASSOCIATED CONTENT

Supporting Information

Details of thermodynamic calculations, comparison spectra, and tables with assignments for vibrational spectroscopy, experimental details for in situ preparation of **1**, results of TGA and DSC measurements of **1**, crystal refinement details, crystal packing figure of **2**, structural parameter comparison tables of **2**, and calculated structures of $[O_3SOSO_2]^{2-}$, $O_3ClOClO_2$, and second conformation of $[(O_2SO)_2SO_2]^{2-}$. CCDC 824802 contains the supplementary crystallographic data for this paper. This material is available free of charge via the Internet at http://pubs.acs.org.

■ AUTHOR INFORMATION

Corresponding Author

*E-mail: passmore@unb.ca. Fax: 1 506 453 4981. Tel.: 1 506 453 4821.

Notes

The authors declare no competing financial interest.

∥E-mail: Mikko.Rautiainen@oulu.fi.

⊥E-mail: tom.whidden@ah2inc.com.

■ ACKNOWLEDGMENTS

We thank NSERC (Natural Sciences and Engineering Research Council) and NBIF (New Brunswick Innovation Foundation) for financial support, Sandra Riley at the University of New Brunswick for assistance with TGA and DSC, Emma Harris for vapor pressure measurements, and Birgit Müller for TGA. ACEnet, the regional high performance computing consortium for universities in Atlantic Canada and CSC-IT Center for Science Ltd. in Finland are acknowledged for providing computational resources.

REFERENCES

(1) Mellor, J. W. *A Comprehensive Treatise on Inorganic and Theoretical Chemistry*; Longmans, Green and Co., Ltd.: London, U.K., 1940; Vol. *X*.
(2) Greenwood, N. N.; Earnshaw, A. *Chemistry of the Elements*; Butterworth-Heinemann, Reed Educational and Professional Publishing, Ltd.: Oxford, Boston, 1984; Vol. *2*, pp 706−721.
(3) Hill, J. C. *J. Chem. Educ.* **1979**, *56*, 593.
(4) Chan, J.; Grein, F. *Comput. Theor. Chem.* **2011**, *966*, 225.
(5) Jansen, M.; Schatte, G.; Tobias, K. M.; Willner, H. *Inorg. Chem.* **1988**, *27*, 1703.
(6) Taylor, P. G.; Beevers, C. A. *Acta Crystallogr.* **1952**, *5*, 341.
(7) Duniz, J. D. *Acta Crystallogr.* **1956**, *9*, 579.
(8) Zachariasen, W. H.; Buckley, H. E. *Phys. Rev.* **1931**, *37*, 1295.
(9) Zachariasen, W. H. *Phys. Rev.* **1932**, *40*, 923.
(10) Barnes, W. H.; Helwig, G. V. *Can. J. Res.* **1931**, *4*, 565.
(11) Zachariasen, W. H. *Z. Kristallogr.* **1934**, *89*, 529.
(12) Goeder, F. P. *Proc. Natl. Acad. Sci. U. S. A.* **1927**, *13*, 793.
(13) Lynton, H.; Truter, M. R. *J. Chem. Soc.* **1960**, 5112.
(14) (a) Eriks, K.; MacGillavry, C. H. *Acta Crystallogr.* **1954**, *7*, 430. (b) Cruickshank, D. W. J. *Acta Crystallogr.* **1964**, *17*, 684.
(15) Zachariasen, W. H.; Mooney, R. C. L. *Z. Kristallogr.* **1934**, *88*, 63.
(16) (a) Jenkins, H. D. B.; Passmore, J.; Glasser, L. *Inorg. Chem.* **1999**, *38*, 3609. (b) Jenkins, H. D. B.; Glasser, L. *Inorg. Chem.* **2003**, *42*, 8702.
(17) Jander, G.; Mesech, H. *Z. Phys. Chem.* **1938**, *A183*, 121.
(18) Baumgarten, P.; Thilo, E. *Ber. Dtsch. Chem. Ges.* **1938**, *71*, 2596.
(19) (a) Logemann, C.; Klüner, T.; Wickleder, M. S. *Angew. Chem., Int. Ed.* **2012**, *51*, 4997. (b) de Vries, R.; Mijlhoff, F. C. *Acta Crystallogr.* **1969**, *B25*, 1696.
(20) Pandey, R.; Biswas, R.; Chakrabarti, T.; Devotta, S. *Crit. Rev. Environ. Sci. Technol.* **2005**, *35*, 571.
(21) (a) Murchie, M.; Passmore, J. *Inorg. Synth.* **1990**, *27*, 332. (b) Murchie, M. P.; Kapoor, R.; Passmore, J.; Schatte, G.; Way, T. *Inorg. Synth.* **1997**, *31*, 102.
(22) Malchus, M.; Jansen, M. *Acta Crystallogr.* **1998**, *B54*, 494.
(23) *CELL_NOW*, V. 2008/2; Bruker AXS, Inc.: Madison, WI.
(24) *SAINT*, 7.23A; Bruker AXS, Inc.; Madison, WI, 2006.
(25) *TWINABS*, 1.05; Bruker Nonius, Inc.: Madison, WI, 2004.
(26) Sheldrick, G. M. *Acta Crystallogr.* **2008**, *A64*, 112.
(27) Brandenburg, K.; Brandt, M. *DIAMOND 3.2h*; Crystal Impact: Bonn, Germany.
(28) Frisch, M. J.; Trucks, G. W.; Schlegel, H. B.; Scuseria, G. E.; Robb, M. A.; Cheeseman, J. R.; Montgomery, Jr., J. A.; Vreven, T.; Kudin, K. N.; Burant, J. C.; Millam, J. M.; Iyengar, S. S.; Tomasi, J.; Barone, V.; Mennucci, B.; Cossi, M.; Scalmani, G.; Rega, N.; Petersson, G. A.; Nakatsuji, H.; Hada, M.; Ehara, M.; Toyota, K.; Fukuda, R.; Hasegawa, J.; Ishida, M.; Nakajima,T.; Honda, Y.; Kitao, O.; Nakai, H.; Klene, M.; Li, X.; Knox, J. E.; Hratchian, H. P.; Cross, J. B.; Bakken, V.; Adamo, C.; Jaramillo, J.; Gomperts, R.; Stratmann, R. E.; Yazyev, O.; Austin, A. J.; Cammi, R.; Pomelli, C.; Ochterski, J. W.; Ayala, P. Y.; Morokuma, K.; Voth, G. A.; Salvador, P.; Dannenberg, J. J.; Zakrzewski, V. G.; Dapprich, S.; Daniels, A. D.; Strain, M. C.; Farkas, O.; Malick, D. K.; Rabuck, A. D.; Raghavachari, K.; Foresman, J. B.; Ortiz, J. V.; Cui, Q.; Baboul, A. G.; Clifford, S.; Cioslowski, J.; Stefanov, B. B.; Liu, G.; Liashenko, A.; Piskorz, P.; Komaromi, I.; Martin, R. L.; Fox, D. J.; Keith, T.; Al-Laham, M. A.; Peng, C. Y.; Nanayakkara, A.; Challacombe, M.; Gill, P. M. W.; Johnson, B.; Chen, W.; Wong, M. W.; Gonzalez, C.; Pople, J. A. *Gaussian 03*, revision E.01; Gaussian, Inc.: Wallingford, CT, 2004.
(29) (a) Becke, A. D. *J. Chem. Phys.* **1993**, *98*, 5648. (b) Perdew, J. P.; Wang, Y. *Phys. Rev. B* **1992**, *45*, 13244.
(30) Zhurko, G. A. *ChemCraft*, 1.6; www.chemcraftprog.com.
(31) Decken, A.; Knapp, C.; Nikiforov, G. B.; Passmore, J.; Rautiainen, J. M.; Wang, X.; Zeng, X. *Chem.—Eur. J.* **2009**, *15*, 6504.
(32) Kumar, A.; McGrady, G. S.; Passmore, J.; Grein, F.; Decken, A. *Z. Anorg. Allg. Chem.* **2012**, *638*, 744.
(33) Glendening, E. D.; Badenhoop, J. K.; Reed, A. E.; Carpenter, J. E.; Bohmann, J. A.; Morales, C. M.; Weinhold, F. *NBO 5.9*; Theoretical Chemistry Institute, University of Wisconsin: Madison, WI, 2012; http://www.chem.wisc.edu/~nbo5.
(34) Degen, I. A.; Newman, G. A. *Spectrochim. Acta* **1993**, *49A*, 859.
(35) Palmer, W. G. *J. Chem. Soc.* **1961**, 1552.
(36) Risberg, E. D.; Eriksson, L.; Mink, J.; Pettersson, L. G. M.; Skripkin, M. Y.; Sandström, M. *Inorg. Chem.* **2007**, *46*, 8332.
(37) Cohen-Addad, C.; Lehmann, M. S.; Becker, P.; Davy, H. *Acta Crystallogr.* **1988**, *B44*, 522.
(38) Richtera, L.; Taraba, J.; Toužin, J. *Collect. Czech. Chem. Commun.* **2006**, *71*, 155.
(39) (a) Reed, A. E.; Weinstock, R. B.; Weinhold, F. *J. Chem. Phys.* **1985**, *83*, 735. (b) Reed, A. E.; Curtiss, L. A.; Weinhold, F. *Chem. Rev.* **1988**, *88*, 899.
(40) Grabowsky, S.; Luger, P.; Buschmann, J.; Schneider, T.; Schirmeister, T.; Sobolev, A. N.; Jayatilaka, D. *Angew. Chem., Int. Ed.* **2012**, *51*, 6776.
(41) Steudel, R.; Steudel, Y. *Eur. J. Inorg. Chem.* **2009**, 1393.
(42) (a) Schmøkel, M. S.; Cenedese, S.; Overgaard, J.; Jørgensen, M. R. V.; Chen, Y.-S.; Gatti, C.; Stalke, D.; Iversen, B. B. *Inorg. Chem.* **2012**, *51*, 8607. (b) Cioslowski, J.; Mixon, S. T. *Inorg. Chem.* **1993**, *32*, 3209. (c) Reed, A.; Schleyer, P. v. R. *J. Am. Chem. Soc.* **1990**, *112*, 1434.
(43) (a) Robinson, E. A. *J. Mol. Struct. (THEOCHEM)* **1989**, *186*, 9. (b) Mayer, I.; Révész, M. *Inorg. Chim. Acta* **1983**, *77*, L205. (c) Cruickshank, D. W. J.; Robinson, E. A. *Spectrochim. Acta* **1966**, *22*, 555. (d) Cruickshank, D. W. J. *J. Chem. Soc.* **1961**, 5486.
(44) (a) Passmore, J.; Rautiainen, J. M. *Eur. J. Inorg. Chem.* **2012**, 6002. (b) Stalke, D. *Chem.—Eur. J.* **2011**, *17*, 9264. (c) Gillespie, R. J.; Silvi, B. *Coord. Chem. Rev.* **2002**, *233−234*, 53. (d) Mo, Y.; Zhang, Y.; Gao, J. *J. Am. Chem. Soc.* **1999**, *121*, 5737.
(45) Sum of charge on SO_2 unit (O5S2O6) is −0.41 in comparison with a neutral SO_2 molecule; therefore 0.41 electrons are transferred from the SO_4 unit (O1O2S1O3O4) to the SO_2 unit (O5S2O6).
(46) (a) Bruna, P. J.; Greer, S.; Passmore, J.; Rautiainen, J. M. *Inorg. Chem.* **2011**, *50*, 1491. (b) Byrd, E. F. C.; Rice, B. M. *J. Phys. Chem. A* **2009**, *113*, 345.
(47) (a) Bond orders were estimated using a variation on Pauling's bond distance-bond order relationship. $D(n') = D1 - 0.997 \log n'$, where n' is the bond order, $D(n')$ is the observed bond length [Å], and D1 is the S−O single bond distance extrapolated (1.70 Å). The constant 0.997 was determined by assuming that the bond order of SO in SOF_4 (bond distance = 1.40 Å) is 2.0. (b) Gillespie, R. J.; Robinson, E. A. *Can. J. Chem.* **1963**, *41*, 2074.
(48) The Cambridge Structural Database version 5.32, accessed in August 2011.
(49) Elschenbroich, C.; Gondrum, R.; Massa, W. *Angew. Chem.* **1985**, *97*, 976.
(50) (a) Perkins, C. W.; Wilson, S. R.; Martin, J. C. *J. Am. Chem. Soc.* **1985**, *107*, 3209. (b) Lam, W. Y.; Duesler, E. N.; Martin, J. C. *J. Am. Chem. Soc.* **1981**, *103*, 127.